CROATICA CHEMICA ACTA CCACAA **73** (4) 923–941 (2000)

ÐISSN-0011-1643
CCA-2692 *Original Scientific Paper*

Reverse Wiener Indices

Alexandru T. Balaban,[a,b,*] *Denise Mills,*[a] *Ovidiu Ivanciuc,*[b] *and Subhash C. Basak* [a,*]

[a] *Natural Resources Research Institute, University of Minnesota-Duluth, 5013 Miller Trunk Highway, Duluth, MN 55811–1442, USA*

[b] *Department of Organic Chemistry, University »Politehnica« of Bucharest, Oficiul 12 CP 243, 78100 Bucharest, Romania*

Received July 19, 1999; revised March 22, 2000; accepted March 29, 2000

By subtracting from the graph diameter all topological distances one obtains a new symmetrical matrix, reverse Wiener ***RW***, with zeroes on the main diagonal, whose sums over rows or columns give rise to new integer-number graph invariants σ_i whose half-sum is a novel topological index (*TI*), the reverse Wiener index Λ. Analytical forms for values of σ_i and Λ of several classes of graphs are presented. Relationships with other *TI*s are discussed. Unlike distance sums, σ_i values increase from the periphery towards the center of the graph, and they are equal to the graph vertex degrees when the diameter of the graph is equal to 2. Structural descriptors computed from the reverse Wiener matrix were tested in a large number of quantitative structure-property relationship models, demonstrating the usefulness of the new molecular matrix.

Key words: molecular graph, molecular matrix, structural descriptor, topological index, reverse Wiener matrix, reverse Wiener index, quantitative structure-property relationships.

INTRODUCTION

A topological index (*TI*) is a number associated with a chemical structure represented by a connected graph (usually a hydrogen-depleted graph) wherein atoms are represented by vertices (points) and covalent bonds by

* Author to whom correspondence should be addressed.

edges (lines) connecting adjacent vertices.[1] The first *TI*s were introduced in the late 40s by Wiener[2–4] and by Platt.[5,6] Since then, many new *TI*s have been added for quantitative structure-property relationship (QSPR) and especially quantitative structure-activity relationship (QSAR) studies.[7–21] Several hundreds of mathematical descriptors derived from molecular graphs were proposed in the literature, but only a few of them were found useful in QSPR models.[22,23]

Wiener's index, denoted by *W*, is defined as the sum of all topological distances in the hydrogen-depleted graph. The topological distance d_{ij} between two graph vertices v_i and v_j is the number of edges along the shortest path between these two vertices. The matrix which has as entries d_{ij} (topological distances) is called the distance matrix $\boldsymbol{D}$ of the graph; it is symmetrical and has zeroes only on its main diagonal. A simple way to compute *W* from the distance matrix of the graph is to add all d_{ij} entries along the row i or column i resulting in a local vertex invariant (LOVI) called the distance sum (or distasum), s_i, of vertex i:

$$s_i = \sum_{j=1}^{N} d_{ij} \quad . \tag{1}$$

Then the Wiener index *W* is the half-sum of all distasums:

$$W = \frac{1}{2} \sum_{i=1}^{N} s_i = \sum_{i=1}^{N} \sum_{j=i}^{N} [\boldsymbol{D}]_{ij} \quad . \tag{2}$$

Like all first-generation *TI*s which are integer numbers based on integer LOVIs, the Wiener index has a fairly large degeneracy, *i.e.* several non-isomorphic graphs can correspond to the same *W* value. In addition, the highest contribution to *W* is made by LOVIs of peripheral vertices which have the largest s_i values. With the aim to remedy these two drawbacks of *W*, research groups in Bucharest[24,25] and in Zagreb[26] introduced independently a different matrix, the reciprocal distance matrix $\boldsymbol{RD}$, whose entries are d_{ij}^{-1} (the reciprocal values of topological distances). The *TI* resulted from an operation similar to that leading to *W* affords a number *H* termed the Harary index,[24–27] that is denoted also *Wi*($\boldsymbol{RD}$). Since it is based on a rational LOVI (sums over rows or columns of d_{ij}^{-1} values in the reciprocal distance matrix), *Wi*($\boldsymbol{RD}$) has a slightly lower degeneracy than *W* and the corresponding LOVIs are highest for the central vertices of the graph.

The present paper starts with the same aim and introduces another type of symmetrical matrix (reverse Wiener matrix, $\boldsymbol{RW}$), yielding LOVIs that are highest for the central graph vertices, and *TI*s which are termed »reverse Wiener indices« denoted by Λ (it would have been appropriate to pro-

pose the letter *M* (because this letter looks like an inverted *W*) but this notation was used[28] for another one of the Zagreb group indices).

Another type of matrix that was independently proposed in Bucharest[29] and in Zagreb[30] is the detour matrix Δ whose entries are the longest paths between every vertex pair.[16,17] Of course, in acyclic graphs there is a single path between any two vertices; therefore the *TI* derived analogously to *W* from the detour matrix and denoted by $Wi(\Delta)$ is identical to *W*; in cyclic graphs, however, $Wi(\Delta)$ differs from *W*.

REVERSE WIENER MATRIX AND DERIVED DESCRIPTORS

The diameter d of a graph is the largest topological distance between any two vertices, *i.e.* the largest d_{ij} value in the distance matrix. Starting from the distance matrix and subtracting from d each d_{ij} value, one obtains a new symmetrical matrix which, like the distance matrix, has zeroes on the main diagonal and, in addition, at least a pair of zeroes off the main diagonal corresponding to the diameter in the distance matrix:

$$[\boldsymbol{RW}]_{ij} = \begin{cases} d - [\boldsymbol{D}]_{ij} & \text{if} \quad i \neq j \\ 0 & \text{if} \quad i = j \end{cases} \tag{3}$$

where $[\boldsymbol{D}]_{ij}$ is the ij-th element of the distance matrix $\boldsymbol{D}$ which is equal to the graph distance between vertices v_i and v_j. Sums over row i or column i of this matrix are LOVIs called reverse-distance sums denoted by σ_i. The half-sum of all σ_i values affords the reverse-Wiener index Λ:

$$\Lambda = \frac{1}{2}\sum_{i=1}^{N} \sigma_i = \sum_{i=1}^{N} \sum_{j=i}^{N} [\boldsymbol{RW}]_{ij} \tag{4}$$

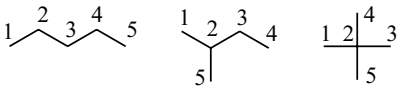

1 **2** **3**

We present below the distance and reverse Wiener matrices, with the corresponding LOVIs s_i and σ_i, for *n*-pentane (**1**), 2-methylbutane (**2**), and 2,2-dimethylpropane (**3**), respectively.

The complementary distance matrix $\boldsymbol{CD} = \boldsymbol{CD}(G)$ of a graph G with N vertices is the square $N \times N$ symmetric matrix whose elements are defined as:[31]

	***D*(1)**					s_i
	1	2	3	4	5	
1	0	1	2	3	4	10
2	1	0	1	2	3	7
3	2	1	0	1	2	6
4	3	2	1	0	1	7
5	4	3	2	1	0	10

	***D*(2)**					s_i
	1	2	3	4	5	
1	0	1	2	3	2	8
2	1	0	1	2	1	5
3	2	1	0	1	2	6
4	3	2	1	0	3	9
5	2	1	2	3	0	8

	***D*(3)**					s_i
	1	2	3	4	5	
1	0	1	2	2	2	7
2	1	0	1	1	1	4
3	2	1	0	2	2	7
4	2	1	2	0	2	7
5	2	1	2	2	0	7

	***RW*(1)**					σ_i
	1	2	3	4	5	
1	0	3	2	1	0	6
2	3	0	3	2	1	9
3	2	3	0	3	2	10
4	1	2	3	0	3	9
5	0	1	2	3	0	6

	***RW*(2)**					σ_i
	1	2	3	4	5	
1	0	2	1	0	1	4
2	2	0	2	1	2	7
3	1	2	0	2	1	6
4	0	1	2	0	0	3
5	1	2	1	0	0	4

	***RW*(3)**					σ_i
	1	2	3	4	5	
1	0	1	0	0	0	1
2	1	0	1	1	1	4
3	0	1	0	0	0	1
4	0	1	0	0	0	1
5	0	1	0	0	0	1

$$[\boldsymbol{CD}]_{ij} = \begin{cases} d + 1 - [\boldsymbol{D}]_{ij} & \text{if} \quad i \neq j \\ 0 & \text{if} \quad i = j . \end{cases} \tag{5}$$

For alkanes and cycloalkanes it can be observed that all entries in the reverse Wiener matrix ***RW*** are lower by 1 than those in the complementary distance matrix ***CD***.

Another matrix that has a certain similarity with ***RW*** and ***CD*** is the distance complement matrix introduced by Randić.[32] The distance complement matrix ***DC*** = ***DC***(G) of a graph G with N vertices is the square $N \times N$ symmetric matrix whose elements are defined as:

$$[\boldsymbol{DC}]_{ij} = \begin{cases} N - [\boldsymbol{D}]_{ij} & \text{if} \quad i \neq j \\ 0 & \text{if} \quad i = j . \end{cases} \tag{6}$$

General formulas for reverse Wiener indices and the corresponding LOVIs. First one should note relationships between the Wiener and reverse Wiener indices as well as their corresponding constituent LOVIs s_i and σ_i, respectively. Since each entry in the ***RW*** matrix is the difference $d - d_{ij}$ and since there are $N - 1$ entries (one being the zero on the main diagonal), we have:

$$\sigma_i = (N - 1)d - s_i \tag{7}$$

$$\Lambda = \frac{1}{2}\sum_{i=1}^{N} \sigma_i = \sum_{i=1}^{N} \sum_{j=i}^{N} [\boldsymbol{RW}]_{ij} = \frac{1}{2} N(N-1)\, d - W . \tag{8}$$

General formulas for a few classes of simple graphs. We shall discuss general formulas for various classes of the simplest graphs. A *complete graph* K_N has an edge between any pair of its vertices, therefore its diameter d is 1, and all its distance sums are $s_i = N - 1$. Thus its Wiener index is $W = \frac{1}{2} N(N - 1)$, and $\Lambda = 0$. Triangles (K_3) and tetrahedra (K_4) are complete graphs of orders 3 and 4, respectively. The complete graph K_5 will be mentioned below in connection with graphs on 5 vertices.

A *star graph* has a central vertex connected to all remaining vertices which are endpoints (vertices of degree 1). Its diameter is $d = 2$. For the center vertex we have $s_i = \sigma_i = N - 1$, whereas for all the other remaining $N - 1$ vertices $s_i = 1 + 2(N - 2) = 2N - 3$, and $\sigma_i = 1$. It is then easy to show that the Wiener index is $W = (N - 1)^2$ and that the reverse-Wiener index is $\Lambda = N - 1$. Propane, isobutane and neopentane are symbolized by hydrogen-depleted graphs of orders $N = 3$, 4, and 5, respectively.

A *linear graph* has diameter $d = N - 1$. It can be shown that $\sigma_i = (N - 1)^2 - s_i$ and that $W = (N^3 - N)/6$. Then it follows that $\Lambda = N(N - 1)(N - 2)/3 = (2N^3 - 6N^2 + 4N)/6$. All normal alkanes (such as *n*-pentane (**1**), presented before) are symbolized by linear graphs.

A $2k$-membered cycloalkane corresponds to a *ring-graph* with order $N = 2k$. It can be shown that for such a graph $W = k^3$. Since the diameter is $d = k$, it follows that the reverse-Wiener index is $\Lambda = k^3 - k^2 = k^2(k - 1)$. For $(2k + 1)$-membered rings, $d = k$ and the formulas are: $W = \frac{1}{2} k(k + 1)(2k + 1)$ and $\Lambda = \frac{1}{2} k(k + 1)(2k - 1)$.

The saturated analogs of *acenes* with h hexagons have $N = 4h + 2$ vertices and a diameter $d = 2h + 1$. Their Wiener numbers are $W = (16h^3 + 36h^2 + 26h + 3)/3$, and the Λ indices are $\Lambda = 2h(16h^2 + 12h - 1)/3$. Further below we shall discuss how one can take into account bond multiplicities (along with the presence of heteroatoms), and this is why here we do not assimilate acenes with their saturated derivatives as it is usually done with Wiener indices.

General considerations about comparisons between the **W** *and* Λ *indices, and between* Λ *and other related indices.* Both indices W and Λ increase with increasing size of graphs. However, W increases faster than Λ for strongly branched graphs such as the star graphs, whereas Λ increases faster than W for less branched graphs such as the linear graphs or saturated acene derivatives. For ring graphs, W and Λ increase similarly with increasing N, but W is always larger than Λ. By design, LOVIs vary differently: central vertices have lower s_i values and higher σ_i values than marginal vertices. This variation of σ_i values is similar to that of LOVIs corresponding to reciprocal distance matrices, and opposite to that of LOVIs derived from the detour matrix.

Degeneracies of **W** *and* Λ *indices and of the corresponding LOVIs* $\mathbf{s_i}$ *and* $\boldsymbol{\sigma_i}$. For the smallest »identity tree« (the hydrogen-depleted graph symbolizing the carbon skeleton of 3-mehylhexane) whose vertices have no equivalence among them, there is no degeneracy in the LOVIs, as one can see from the values of σ_i and s_i reported in Figure 1. However, each of the four identity graphs with six vertices (mono-, bi- and tricyclic graphs) of Figure 2 has at least one pair of non-equivalent vertices with the same LOVI.

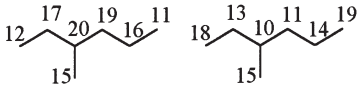

Figure 1. Identity tree with LOVIs: σ_i (left) and s_i (right).

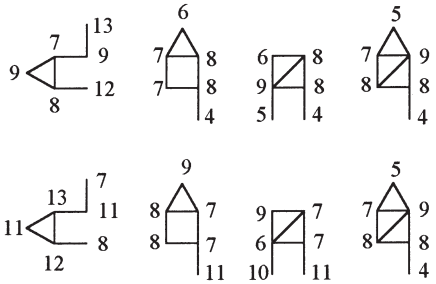

Figure 2. Identity graphs with degenerate LOVIs: s_i (upper row) and σ_i (lower row).

All acyclic graphs with 5 vertices, namely compounds **1**–**3**, were presented with their matrices. In Figure 3 one can see all cyclic graphs **4**–**20** with 5 vertices (except for the complete graph K_5 which being one of the two fundamental Kuratowski non-planar graphs cannot be embedded on a plane without crossing edges). In Table I we present for the molecular graphs **4**–**20** the graph diameter d, the Wiener index W, and the reverse Wiener index Λ. It is easy to prove that for all graphs with $d = 2$ the vertex degrees $\deg_i$ are identical to the σ_i LOVIs.

The degeneracy of W and Λ indices is similar when their graphs have the same order and diameter because they are related to each other by the simple relationship (7). One can observe in Table I that indeed W and Λ have similar degeneracies. Like W, the smallest alkanes with degenerate Λ indices are two pairs of heptane isomers. However, Λ indices have in general lower degeneracies than W because in some cases when two graphs have the same N and W values, their diameters differ; such is the case of 3,3-dime-

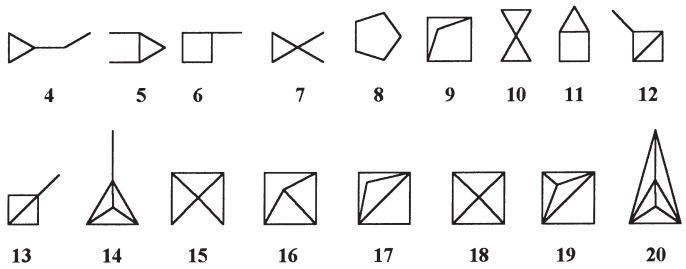

Figure 3. All monocyclic through pentacyclic graphs with five vertices.

TABLE I

Graph diameter, Wiener and reverse Wiener indices for the molecular graphs **4**–**20** from Figure 3

G	d	W	Λ
4	3	17	13
5	3	16	14
6	3	16	14
7	3	15	5
8	2	15	5
9	2	14	6

G	d	W	Λ
10	2	14	6
11	2	14	6
12	3	15	15
13	2	14	6
14	2	13	7
15	2	13	7

G	d	W	Λ
16	2	13	7
17	2	13	7
18	2	12	8
19	2	12	8
20	2	12	8

thylheptane ($W = 98$, $\Lambda = 118$) and 2,2,5-trimethylhexane ($W = 98$, $\Lambda = 82$), or of 4,4-dimethylheptane ($W = 96$, $\Lambda = 84$) and 2,3,5-trimethylhexane ($W = 96$, $\Lambda = 120$).

The advantage of Λ indices over W is that for a series of isomers (such as the alkanes presented in Table II) the Λ indices have a wider range of variation than the Wiener indices. At the same time, since this fact leads to overlapping ranges of variation, it is advisable for QSAR/QSPR studies to include a parameter such as N which is a strict measure for the size of the graph. A drawback of Λ indices is that for isomers with the same diameter d, Λ increases with increasing branching, contrary to the general trend for Λ indices.

Presence of multiple bonds and/or heteroatoms. In the distance matrix one has to input as $1/b$ the topological distance between two atoms connected by a multiple bond with bond order b (where $b = 1$ for single bonds, 2 for double bonds, 3 for triple bonds and 1.5 for aromatic bonds). Then the graph distances and the graph diameter will result as rational numbers instead of integer numbers. The formulas (6) and (7) hold for taking into account bond multiplicities. It should be recalled that chemical-topological dis-

TABLE II

Structure of alkanes and cycloalkanes, number of carbon atoms N, graph diameter d, reverse Wiener index Λ, experimental normal boiling temperature t_b, t_b computed with formula (8), and residual

No	Compound	N	d	Λ	t_b		
					exp	calc	res
1	Propane	3	2	2	–42.1	–27.8	–14.3
2	*n*-Butane	4	3	8	–0.5	0.6	–1.1
3	2-Methylpropane	4	2	3	–11.7	0.0	–11.7
4	*n*-Pentane	5	4	20	36.1	29.7	6.4
5	2-Methylbutane	5	3	12	27.9	28.7	–0.9
6	2,2-Dimethylpropane	5	2	4	9.5	27.8	–18.3
7	*n*-Hexane	6	5	40	68.7	59.7	9.1
8	2-Methylpentane	6	4	28	60.3	58.3	2.0
9	3-Methylpentane	6	4	29	63.3	58.4	4.9
10	2,2-Dimethylbutane	6	3	17	49.7	57.0	–7.2
11	2,3-Dimethylbutane	6	3	16	58.0	58.6	–0.6
12	*n*-Heptane	7	6	70	98.4	90.8	7.6
13	2-Methylhexane	7	5	53	90.1	88.8	1.2
14	3-Methylhexane	7	5	55	91.9	89.1	2.8
15	3-Ethylpentane	7	4	36	93.5	86.9	6.6
16	2,2-Dimethylpentane	7	4	38	79.2	87.1	–7.9
17	2,3-Dimethylpentane	7	4	38	89.8	87.1	2.7
18	2,4-Dimethylpentane	7	4	36	80.5	86.9	–6.4
19	3,3-Dimethylpentane	7	4	40	86.1	87.3	–1.3
20	2,2,3-Trimethylbutane	7	3	21	80.9	86.3	–5.4
21	*n*-Octane	8	7	112	125.7	123.4	2.3
22	2-Methylheptane	8	6	89	117.7	120.7	–3.1
23	3-Methylheptane	8	6	92	118.9	121.1	–2.1
24	4-Methylheptane	8	6	93	117.7	121.2	–3.5
25	3-Ethylhexane	8	5	68	118.5	118.3	0.3
26	2,2-Dimethylhexane	8	5	69	106.8	118.4	–11.5
27	2,3-Dimethylhexane	8	5	70	115.6	118.5	–2.9
28	2,4-Dimethylhexane	8	5	69	109.4	118.4	–9.0
29	2,5-Dimethylhexane	8	5	66	109.1	118.0	–8.9
30	3,3-Dimethylhexane	8	5	73	112.0	118.8	–6.9
31	3,4-Dimethylhexane	8	5	72	117.7	118.7	–1.0
32	3-Ethyl-2-methylpentane	8	4	45	115.7	115.6	0.1
33	3-Ethyl-3-methylpentane	8	4	48	118.3	115.9	2.3
34	2,2,3-Trimethylpentane	8	4	49	109.8	116.1	–6.2
35	2,2,4-Trimethylpentane	8	4	46	99.2	115.7	–16.5
36	2,3,3-Trimethylpentane	8	4	50	114.8	116.2	–1.4
37	2,3,4-Trimethylpentane	8	4	47	113.5	115.8	–2.3
38	2,2,3,3-Tetramethylbutane	8	3	26	106.5	113.4	–6.9
39	Cyclobutane	4	2	4	12.0	0.1	11.9
40	Ethylcyclobutane	6	4	31	70.7	58.6	12.1

TABLE II (continued)

No	Compound	N	d	Λ	t_b		
					exp	calc	res
41	Methylcyclobutane	5	3	14	36.3	29.0	7.3
42	Butylcyclohexane	10	7	182	181.6	186.9	–5.3
43	Isopropylcyclohexane	9	5	92	154.8	148.7	6.1
44	*s*-Butylcyclohexane	10	6	95	179.3	176.8	2.5
45	*t*-Butylcyclohexane	10	5	111	171.5	178.6	–7.1
46	1-Methyl-4-ethylcyclohexane	9	6	126	150.0	152.7	–2.7
47	Propylcyclohexane	9	6	122	156.7	152.2	4.5
48	1,1,3-Trimethylcyclohexane	9	4	62	139.0	145.2	–6.2
49	1,2,4-Trimethylcyclohexane	9	5	98	144.8	149.4	–4.6
50	1,2-Diethylcyclopentane	9	5	93	153.6	148.9	4.7
51	1,1-Dimethylcyclopentane	7	3	24	87.5	85.5	2.0
52	1,2-Dimethylcyclopentane	7	3	23	95.5	85.4	10.1
53	Ethylcyclopentane	7	4	45	103.5	87.9	15.6
54	Methylcyclopentane	6	3	19	71.8	57.2	14.6
55	1-Methyl-2-propylcyclopentane	9	5	90	152.6	148.5	4.1
56	Cyclopropane	3	1	0	–32.7	–28.0	–4.7
57	1,1-Dimethylcyclopropane	5	2	5	20.6	27.9	–7.3
58	1,2-Dimethylcyclopropane	5	3	14	33.0	27.8	5.2
59	Ethylcyclopropane	5	3	13	34.5	28.8	5.7
60	Methylcyclopropane	4	2	4	0.7	0.1	0.6
61	1,1,2-Trimethylcyclopropane	6	3	19	52.6	57.2	–4.6
62	1,4-Dimethylcyclohexane	8	5	78	121.8	119.4	2.4
63	Ethylcyclohexane	8	5	76	131.8	119.2	12.6
64	Propylcyclopentane	8	5	73	131.0	118.8	12.2
65	Isopropylcyclopentane	8	4	50	126.4	116.2	10.2
66	1,1,2-Trimethylcyclopentane	8	3	28	113.5	113.6	–0.1
67	1,1,3-Trimethylcyclopentane	8	4	54	104.9	116.6	–11.7
68	1,1-Dimethylcyclohexane	8	4	53	119.5	116.5	3.0
69	1,2-Dimethylcyclohexane	8	4	52	126.6	116.4	10.2
70	1,3-Dimethylcyclohexane	8	4	51	122.3	116.3	6.0

tances b^{-4} were found[33] to reflect the actual relative bond lengths of multiple bonds much better than b^{-1}.

The presence of heteroatoms can be treated variously,[15,34–36] for instance by including information on the nature of these heteroatoms *via* their relative electronegativity or covalent radius, multiplying their σ_i values by the corresponding data relative to those of carbon atoms,[34] and in addition by an adjustable parameter which is to be determined from the properties of the set of compounds used in the QSAR or QSPR study.

QSPR model for the normal boiling temperatures of saturated hydrocarbons. Because the boiling temperatures at normal pressure (t_b) are among the properties that are determined with the highest accuracy, many new topological indices are validated by seeing whether they can be correlated satisfactorily with t_b.[37–55] Among the set of compounds that were thus used for testing, alkanes were the most frequently used.[37–39] Studies involving cycloalkanes,[39] haloalkanes,[43–46] oxygen and sulfur analogues of alkanes devoid of hydrogen bonding (*i.e.* oxa- and thia-alkanes)[47] have also been reported.

In Table II we present the results of the biparametric correlation between t_b of 38 alkanes plus 32 cycloalkanes using the following equation:

$$t_b = 0.1166\ (\pm\ 0.0471)\Lambda + 27.67\ (\pm\ 1.03)N - 111.02\ (\pm\ 5.56) \qquad (9)$$
$$r^2 = 0.9769 \quad s = 7.62\ ^\circ\mathrm{C} \quad F = 1416\ .$$

When each of the two above variables was used in single-parameter correlations, the results were:

$$t_b = 28.91\ (\pm 0.58)N - 120.31\ (\pm 4.24) \qquad (10)$$
$$r^2 = 0.9748 \quad s = 7.91\ ^\circ\mathrm{C} \quad F = 2630$$

$$t_b = 1.1780\ (\pm\ 0.0872)\Lambda + 31.76\ (\pm\ 5.42) \qquad (11)$$
$$r^2 = 0.7286 \quad s = 25.9\ ^\circ\mathrm{C} \quad F = 182\ .$$

Evidently, most of the variance in t_b of saturated hydrocarbons is accounted for by the number N of carbon atoms, but *TI*s (and Λ in particular) improve the correlation.

QSPR models for alkane properties. In this section we present a more complete evaluation of topological indices derived from the reverse Wiener matrix. The QSPR models were developed for a data set consisting of 134 alkanes between C_6 and C_{10}, for the following six physical properties:[51] t_b, boiling temperature at normal pressure / °C; C_p, molar heat capacity at 300 K / J K^{-1} mol^{-1}; $\Delta_f G^\circ_{300}$ (g), standard Gibbs energy of formation in the gas phase at 300 K / kJ mol^{-1}; $\Delta_{vap}H_{300}$, vaporization enthalpy at 300 K / kJ mol^{-1}; $n_D{}^{25}$, refractive index at 25 °C; ρ, density at 25 °C / kg m^{-3}. The value of the refractive index of 2,2,3,3-tetramethylbutane is missing, while the reported density of this compound, 821.70 kg m^{-3}, is too high when compared with the density of similar alkanes and it was not considered in the computation of the density QSPR models. As it is known, there are 142 constitutional isomers for these alkanes, but data for all six properties are missing for the following eight of them: *n*-hexane, *n*-nonane, *n*-decane, 2-methyl-

nonane, 3-methylnonane, 4-methylnonane, 5-methylnonane, 3-ethyl-2,4-dimethylhexane. Three Wiener-type indices from three molecular matrices were computed for all alkanes in the data base: W from the distance matrix $\boldsymbol{D}$, $Wi(\boldsymbol{RD})$ from the reciprocal distance matrix $\boldsymbol{RD}$, and Λ from the reverse Wiener matrix $\boldsymbol{RW}$.

The first test considers monoparametric QSPR models of the six properties obtained for the set of 34 nonanes in the data base. The QSPR equation developed for an isomeric series of alkanes models only the branching effect on the investigated properties, because the size is constant.

TABLE III

Statistical indices of the monoparametric QSPR models for the six alkane properties developed for the set of 34 nonane isomers. The MLR equations have the general form: $P = a_0 + a_1\mathbf{SD}$.

SD	a_0	a_1	r	s	F
(1) boiling temperature at normal pressure, t_b / °C					
W	1.32076e+02	5.41250e–02	0.0727	5.99	0.2
$Wi(\boldsymbol{RD})$	1.57187e+02	–1.10628e+00	–0.1125	5.97	0.4
Λ	1.32440e+02	5.16607e–02	0.2301	5.84	1.8
(2) molar heat capacity at 300 K, C_p / J K^{-1} mol^{-1}					
W	2.20969e+02	–8.74038e–02	–0.1934	3.58	1.2
$Wi(\boldsymbol{RD})$	1.96106e+02	9.15039e–01	0.1533	3.60	0.8
Λ	2.14465e+02	–2.01675e–02	–0.1480	3.60	0.7
(3) standard Gibbs energy of formation in the gas phase at 300 K, $\Delta_f G^\circ{}_{300}$ (g) / kJ mol^{-1}					
W	9.74336e+01	–7.28077e–01	–0.8147	4.18	63.1
$Wi(\boldsymbol{RD})$	–1.41436e+02	9.38664e+00	0.7955	4.37	55.1
Λ	4.71375e+01	–2.09551e–01	–0.7779	4.53	49.0
(4) vaporization enthalpy at 300 K, $\Delta_{vap}H_{300}$ / kJ mol^{-1}					
W	2.34270e+01	1.47433e–01	0.7817	0.95	50.3
$Wi(\boldsymbol{RD})$	7.41091e+01	–2.02918e+00	–0.8148	0.88	63.2
Λ	3.39150e+01	3.91916e–02	0.6894	1.10	29.0
(5) refractive index at 25 °C, n_D^{25}					
W	1.46644e+00	–6.09712e–04	–0.7680	0.0041	46.0
$Wi(\boldsymbol{RD})$	1.26955e+00	7.68607e–03	0.7333	0.0044	37.2
Λ	1.42120e+00	–1.42059e–04	–0.5937	0.0052	17.4
(6) density at 25 °C, ρ / kg m^{-3}					
W	8.51898e+02	–1.31689e+00	–0.7666	8.89	45.6
$Wi(\boldsymbol{RD})$	4.29691e+02	1.64310e+01	0.7244	9.55	35.3
Λ	7.55141e+02	–3.17172e–01	–0.6126	10.95	19.2

In Table III we present the coefficients of the QSPR model $P = a_0 + a_1\mathbf{SD}$, where P is the property and **SD** the structural descriptor, and the corresponding statistical indices r, s, and F. An inspection of these results shows that none of the three indices is able to model the boiling temperature and molar heat capacity of the nonanes. For the remaining four properties we have obtained significant correlations with all descriptors; W correlates best with the standard Gibbs energy of formation, refractive index, and density, while $Wi(\boldsymbol{RD})$ is the top index for the modeling of the vaporization enthalpy. The reverse Wiener index Λ gives QSPR models comparable with those obtained with the W and $Wi(\boldsymbol{RD})$ indices, but the statistical indices show that constantly these equations are on the third place.

In Table IV we present the QSPR models obtained in a second test, in which we have considered all 69 decanes in the data base. The examination of these results shows a great similarity with the results obtained for nonanes. All QSPR models for the boiling temperature and molar heat capacity of the decanes are of poor statistical quality, while for the other four properties we have obtained good correlations. The best equations are obtained with the same indices identified in the case of nonanes: W for the standard Gibbs energy of formation, refractive index, and density, while $Wi(\boldsymbol{RD})$ is the best index for the vaporization enthalpy. Although the reverse Wiener index Λ gives significant QSPR models for the last four alkane properties, they are always on the third place, after those obtained with W and $Wi(\boldsymbol{RD})$.

The third test considers monoparametric QSPR models of the six properties obtained for all 134 alkanes in the data base. To the set of three topological indices we have added N, the number of carbon atoms, representing a size parameter. The use of the number of carbon atoms offers the possibility to decide if a particular topological index provides better correlations than a simple descriptor like N. The results reported in Table V show that N gives the best correlations with the boiling temperature and molar heat capacity, while the remaining four properties are modeled best with Wiener-type indices computed from the $\boldsymbol{D}$ and $\boldsymbol{RD}$ matrices: W for the vaporization enthalpy, and $Wi(\boldsymbol{RD})$ for the standard Gibbs energy of formation, refractive index, and density. The reverse Wiener index Λ gives significant QSPR models for the boiling temperature, molar heat capacity, and vaporization enthalpy, but again the statistical indices show that constantly these equations are on the last place.

In Table VI we present the QSPR models with two descriptors with the general form: $P = a_0 + a_1N + a_2\mathbf{SD}$. Obviously, in the case of the boiling temperature and molar heat capacity the addition of a topological index does not improve the correlation. The QSPR models for the remaining four prop-

TABLE IV

Statistical indices of the monoparametric QSPR models for the six alkane properties developed for the set of 69 decane isomers. The MLR equations have the general form: $P = a_0 + a_1\mathbf{SD}$.

SD	a_0	a_1	r	s	F
(1) boiling temperature at normal pressure, t_b / °C					
W	1.75008e+02	–1.25760e–01	–0.2090	5.95	3.1
$Wi(\boldsymbol{RD})$	1.27330e+02	1.47842e+00	0.1706	5.99	2.0
Λ	1.59210e+02	–2.12718e–03	–0.0114	6.08	0.0
(2) molar heat capacity at 300 K, C_p / J K^{-1} mol^{-1}					
W	2.29274e+02	4.59573e–02	0.0957	4.83	0.6
$Wi(\boldsymbol{RD})$	2.58898e+02	–1.11093e+00	–0.1607	4.79	1.8
Λ	2.32503e+02	2.06689e–02	0.1391	4.81	1.3
(3) standard Gibbs energy of formation in the gas phase at 300 K, $\Delta_f G^\circ_{300}$ (g) / kJ mol^{-1}					
W	1.57251e+02	–9.23260e–01	–0.8379	6.08	157.9
$Wi(\boldsymbol{RD})$	–2.38890e+02	1.30107e+01	0.8200	6.38	137.5
Λ	7.19181e+01	–2.55293e–01	–0.7484	7.39	85.3
(4) vaporization enthalpy at 300 K, $\Delta_{vap}H_{300}$ / kJ mol^{-1})					
W	2.58281e+01	1.19941e–01	0.7342	1.12	78.3
$Wi(\boldsymbol{RD})$	8.11932e+01	–1.87275e+00	–0.7961	1.00	115.9
Λ	3.69949e+01	3.25300e–02	0.6432	1.26	47.3
(5) refractive index at 25 °C, n_D^{25}					
W	1.49424e+00	–5.97134e–04	–0.8093	0.0044	127.2
$Wi(\boldsymbol{RD})$	1.23520e+00	8.54722e–03	0.8044	0.0044	122.9
Λ	1.43541e+00	–1.36667e–04	–0.5983	0.0060	37.3
(6) density at 25 °C, ρ / kg m^{-3}					
W	9.02324e+02	–1.24386e+00	–0.8361	8.25	155.6
$Wi(\boldsymbol{RD})$	3.70822e+02	1.74258e+01	0.8134	8.75	131.0
Λ	7.78933e+02	–2.78038e–01	–0.6036	11.99	38.4

erties are significantly improved by the use of a biparametric equation. The models that contain N and W give the best results for the standard Gibbs energy of formation, refractive index, and density, while the vaporization enthalpy is computed best by the model which contains N and $Wi(\boldsymbol{RD})$. The QSPR models containing the reverse Wiener index Λ give good correlations, but they are constantly ranked on the last place.

However, it is not possible to draw definite conclusions on the utility of the reverse Wiener matrix from QSPR models computed only with the reverse Wiener index Λ. Powerful structural descriptors for QSPR and QSAR studies were recently proposed,[14–16] such as the spectral operators **MinSp**

TABLE V

Statistical indices of the monoparametric QSPR models for the six alkane properties developed for the set of 134 alkanes C_6–C_{10}. The MLR equations have the general form: $P = a_0 + a_1$**SD**.

SD	a_0	a_1	r	s	F
(1) boiling temperature at normal pressure, t_b / °C					
N	–7.89057e+01	2.38593e+01	0.9727	6.19	2314.7
W	5.61843e+01	8.04704e–01	0.9200	10.44	727.2
Wi(***RD***)	4.36055e+00	7.25382e+00	0.9522	8.14	1281.9
Λ	9.19692e+01	4.66784e–01	0.7358	18.04	155.8
(2) molar heat capacity at 300 K, C_p / J K^{-1} mol^{-1}					
N	3.68919e+00	2.31610e+01	0.9870	4.10	4977.7
W	1.34137e+02	7.87790e–01	0.9415	8.59	1030.1
Wi(***RD***)	8.43197e+01	7.05216e+00	0.9677	6.43	1943.9
Λ	1.70291e+02	4.45982e–01	0.7349	17.28	155.0
(3) standard Gibbs energy of formation in the gas phase at 300 K, $\Delta_f G^\circ_{300}$ (g) / kJ mol^{-1}					
N	–6.98957e+01	1.08960e+01	0.8008	8.85	236.0
W	–1.80935e+00	3.05788e–01	0.6303	11.47	87.0
Wi(***RD***)	–3.86365e+01	3.67569e+00	0.8699	7.29	410.5
Λ	1.89608e+01	1.07045e–01	0.3042	14.08	13.5
(4) vaporization enthalpy at 300 K, $\Delta_{vap}H_{300}$ / kJ mol^{-1}					
N	4.19465e+00	3.70044e+00	0.9303	1.58	849.5
W	2.39338e+01	1.36507e–01	0.9625	1.17	1659.8
Wi(***RD***)	1.82633e+01	1.06308e+00	0.8606	2.20	376.9
Λ	2.91761e+01	8.73040e–02	0.8487	2.28	339.9
(5) refractive index at 25 °C, n_D^{25}					
N	1.30795e+00	1.10360e–02	0.8751	0.0066	428.3
W	1.37508e+00	3.27253e–04	0.7246	0.0094	144.8
Wi(***RD***)	1.34197e+00	3.59759e–03	0.9205	0.0053	727.5
Λ	1.39366e+00	1.50562e–04	0.4578	0.0122	34.7
(6) density at 25 °C, ρ / kg m^{-3}					
N	5.36027e+02	2.08349e+01	0.8545	13.75	354.4
W	6.64045e+02	6.05436e–01	0.6933	19.07	121.3
Wi(***RD***)	5.99459e+02	6.83462e+00	0.9045	11.29	589.2
Λ	6.99283e+02	2.70179e–01	0.4249	23.96	28.9

and **MaxSp**,[14,27,35] the Ivanciuc-Balaban operator **IB**,[19,35] and the information-theoretic operators **U**, **V**, **X**, and **Y**.[59–61] In a comparative study we have computed these structural descriptors from four molecular matrices, namely the distance ***D***, reciprocal distance ***RD***, reverse Wiener ***RW***, and reciprocal

TABLE VI

Statistical indices of the biparametric QSPR models for the six alkane properties developed for the set of 134 alkanes C_6–C_{10}. The MLR equations have the general form: $P = a_0 + a_1N + a_2$**SD**.

SD	a_0	a_1	a_2	r	s	F
(1) boiling temperature at normal pressure, t_b / °C						
W	–8.94748e+01	2.58599e+01	–7.47941e–02	0.9730	6.17	1163.6
Wi(***RD***)	–8.80419e+01	2.66552e+01	–8.83326e–01	0.9729	6.19	1158.9
Λ	–7.52488e+01	2.32053e+01	2.28650e–02	0.9730	6.18	1162.0
(2) molar heat capacity at 300 K, C_p (J K^{-1} mol^{-1})						
W	3.82198e+00	2.31358e+01	9.39654e–04	0.9870	4.11	2470.0
Wi(***RD***)	–1.91531e+00	2.48760e+01	–5.41864e–01	0.9871	4.10	2488.4
Λ	4.71755e+00	2.29771e+01	6.42994e–03	0.9870	4.11	2475.0
(3) standard Gibbs energy of formation in the gas phase at 300 K, $\Delta_f G^\circ_{300}$ (g) / kJ mol^{-1}						
W	–1.71303e+02	3.00914e+01	–7.17624e–01	0.9159	5.96	340.8
Wi(***RD***)	3.71533e+01	–2.18629e+01	1.03499e+01	0.9186	5.86	353.9
Λ	–1.05707e+02	1.73005e+01	–2.23914e–01	0.9081	6.21	308.0
(4) vaporization enthalpy at 300 K, $\Delta_{vap}H_{300}$ / kJ mol^{-1}						
W	2.08719e+01	5.43594e–01	1.18019e–01	0.9633	1.16	844.5
Wi(***RD***)	–1.61998e+01	9.94151e+00	–1.97181e+00	0.9755	0.95	1285.8
Λ	1.00272e+01	2.65735e+00	3.64687e–02	0.9604	1.21	778.8
(5) refractive index at 25 °C, n_D^{25}						
W	1.23050e+00	2.57545e–02	–5.52542e–04	0.9490	0.0043	588.6
Wi(***RD***)	1.38161e+00	–1.13884e–02	7.06758e–03	0.9352	0.0049	453.0
Λ	1.28678e+00	1.48583e–02	–1.35163e–04	0.9181	0.0054	348.6
(6) density at 25 °C, ρ / kg m^{-3}						
W	3.70513e+02	5.22859e+01	–1.18069e+00	0.9459	8.62	552.3
Wi(***RD***)	6.88474e+02	–2.55788e+01	1.46283e+01	0.9245	10.13	382.3
Λ	4.91226e+02	2.89228e+01	–2.86008e–01	0.9069	11.20	301.0

reverse Wiener ***RRW*** matrices.[62] Using the same data base of 134 alkanes and six properties, we have found that the molar heat capacity, standard Gibbs energy of formation and vaporization enthalpy are best modeled by QSPR equation containing *TI*s derived from ***RW*** and ***RRW***:

$$C_p = 7.0528(\pm0.5476) + 1.6605(\pm0.1289)M_W +$$
$$+ 0.308320(\pm0.002394)\mathbf{Ho}(\boldsymbol{RRW}) - 0.44721(\pm0.03472)\mathbf{Y}(\boldsymbol{RRW})$$
$$r = 0.9883 \quad s = 3.92 \quad F = 1817.4$$

$$\Delta_f G^\circ_{300} = -146.290(\pm 22.465) + 31.1837(\pm 4.789)\mathbf{IB}(\boldsymbol{D}) + 3.6879(\pm 0.5663)\mathbf{IB}(\boldsymbol{RW}) + 4.8087(\pm 0.7384)\mathbf{V}(\boldsymbol{RD})$$
$$r = 0.9564 \quad s = 4.35 \quad F = 464.6$$

$$\Delta_{vap} H_{300} = -10.1766(\pm 0.7470) + 6.6102(\pm 0.4852)\mathbf{MaxSp}(\boldsymbol{RD}) + 1.6844(\pm 0.1236)\mathbf{V}(\boldsymbol{RD}) + 0.71313(\pm 0.05235)\mathbf{X}(\mathbf{RW})$$
$$r = 0.9895 \quad s = 0.63 \quad F = 2033.4$$

In the QSPR equation that models the molar heat capacity, M_W is the molecular weight and **Ho**(***RRW***) is the Hosoya index[21,63] representing the sum of the coefficients of the characteristic polynomial[64] computed from the ***RRW*** matrix. The above three models demonstrate the utility of the new molecular matrix in the computation of topological indices with good correlational power.

CONCLUDING REMARKS

Molecular graph descriptors represent valuable structural descriptors that can be used with success in developing QSPR and QSAR models; in such structure-property studies, graph descriptors can be used in conjunction with other classes of structural descriptors, such as constitutional, geometrical, electrostatic, and quantum descriptors. In the present study we have defined a new molecular matrix derived from graph distances, namely the reverse Wiener matrix ***RW***, and a Wiener-type index derived from it, the reverse Wiener index Λ. The new topological index was tested in a QSPR model for the normal boiling temperature of a set of alkanes and cycloalkanes. A comparative study was performed for a set of 134 alkanes between C_6 and C_{10}, with Wiener-type indices computed from the distance ***D***, reciprocal distance ***RD***, and reverse Wiener ***RW*** matrices. The data base contains experimental values for six alkane properties: normal boiling temperature, molar heat capacity, standard Gibbs energy of formation, vaporization enthalpy, refractive index, and density. Although the reverse Wiener index Λ gave significant correlations for these properties, when used in monoparametric equations its performances were lower than of the Wiener-type indices derived from the distance and reciprocal distance matrices. However, an extended study that used a larger set of structural descriptors demonstrated that topological indices computed from the reverse Wiener matrix ***RW*** and the reciprocal reverse Wiener matrix ***RRW*** give better QSPR models than the topological indices derived from the ***D*** and ***RD*** matrices. The results obtained in these QSPR investigations demonstrate the utility of the reverse Wiener matrix in computing useful molecular descriptors.

REFERENCES

1. J. Devillers and A. T. Balaban (Eds.), *Topological Indices and Related Descriptors in QSAR and QSPR,* Gordon and Breach, The Netherlands, 1999.
2. H. Wiener, *J. Am. Chem. Soc.* **69** (1947) 17–20.
3. H. Wiener, *J. Am. Chem. Soc.* **69** (1947) 2636–2638.
4. H. Wiener, *J. Phys. Chem*. **52** (1948) 425–430.
5. J. R. Platt, *J. Chem. Phys.* **15** (1947) 419–420.
6. J. R. Platt, *J. Phys. Chem*. **56** (1952) 328–336.
7. A. T. Balaban, I. Motoc, D. Bonchev, and O. Mekenyan, in: M. Charton and I. Motoc (Eds.), *Steric Effects in Drug Design, Topics Curr. Chem.,* Springer, Berlin, **114** (1981) 21.
8. N. Trinajstić, *Chemical Graph Theory,* CRC Press, Boca Raton, 1992, Chapter 10.
9. L. B. Kier and L. H. Hall, *Molecular Connectivity in Chemistry and Drug Research,* Academic Press, New York, 1976; *Molecular Connectivity in Structure-Activity Analysis,* Wiley, New York, 1986; *Molecular Structure Description: The Electrotopological State*, Academic Press, New York, 1999.
10. D. Bonchev, *Information Theoretic Indices for Characterization of Chemical Structures,* Research Studies Press, Chichester, 1983.
11. A. T. Balaban, A. Chiriac, I. Motoc, and Z. Simon*, Steric Fit in Quantitative Structure-Activity Relations,* Lecture Notes in Chemistry No. 15, Springer, Berlin, 1980.
12. S. C. Basak, G. J. Niemi, and G. D. Veith, in: D. H. Rouvray (Ed.), *Computational Chemical Graph Theory,* Nova Science Publishers, New York, 1990, p. 201.
13. M. I. Stankevich, I. V. Stankevich, and N. S. Zefirov, *Russ. Chem. Rev.* **57** (1988) 191.
14. O. Ivanciuc and A. T. Balaban, *The Graph Description of Chemical Structures*, in: J. Devillers and A. T. Balaban (Eds.), *Topological Indices and Related Descriptors in QSAR and QSPR*, Gordon and Breach Science Publishers, The Netherlands, 1999, pp. 59–167.
15. O. Ivanciuc, T. Ivanciuc, and A. T. Balaban, *Vertex- and Edge-Weighted Molecular Graphs and Derived Structural Descriptors*, in: J. Devillers and A. T. Balaban (Eds.), *Topological Indices and Related Descriptors in QSAR and QSPR*, Gordon and Breach Science Publishers, The Netherlands, 1999, pp. 169–220.
16. O. Ivanciuc and T. Ivanciuc, *Matrices and Structural Descriptors Computed from Molecular Graph Distances*, in: J. Devillers and A. T. Balaban (Eds.), *Topological Indices and Related Descriptors in QSAR and QSPR*, Gordon and Breach Science Publishers, The Netherlands, 1999, pp. 221–277.
17. S. Nikolić, N. Trinajstić, and Z. Mihalić, *The Detour Matrix and the Detour Index*, in: J. Devillers and A. T. Balaban (Eds.), *Topological Indices and Related Descriptors in QSAR and QSPR*, Gordon and Breach Science Publishers, The Netherlands, 1999, pp. 279–306.
18. E. Estrada, *Novel Strategies in the Search of Topological Indices*, in: J. Devillers and A. T. Balaban (Eds.), *Topological Indices and Related Descriptors in QSAR and QSPR*, Gordon and Breach Science Publishers, The Netherlands, 1999, pp. 403–453.
19. O. Ivanciuc, T. Ivanciuc, and M. V. Diudea, *SAR QSAR Environ. Res*. **7** (1997) 63–87.
20. M. V. Diudea, *Croat. Chem. Acta* **72** (1999) 835–851.

21. O. Ivanciuc, *Rev. Roum. Chim*. **44** (1999) 519–528.
22. M. Randić, *Croat. Chem. Acta* **66** (1993) 289–312.
23. M. Randić, Z. Mihalić, S. Nikolić, and N. Trinajstić, *Croat. Chem. Acta* **66** (1993) 411–434.
24. T. S. Balaban, P. A. Filip, and O. Ivanciuc, *J. Math. Chem*. **11** (1992) 79–105.
25. O. Ivanciuc, T. S. Balaban, and A. T. Balaban, *J. Math. Chem.* **12** (1993) 309–318.
26. D. Plavšić, S. Nikolić, N. Trinajstić, and Z. Mihalić, *J. Math. Chem.* **12** (1993) 235–250.
27. M. V. Diudea, O. Ivanciuc, S. Nikolić, and N. Trinajstić, *MATCH (Commun. Math. Comput. Chem.)* **35** (1997) 41–64.
28. I. Gutman, B. Ruščić, N. Trinajstić, and C. F. Wilcox, Jr., *J. Chem. Phys*. **62** (1975) 3399–3405.
29. O. Ivanciuc and A. T. Balaban, *MATCH (Commun. Math. Chem.)* **30** (1994) 141–152.
30. D. Amić and N. Trinajstić, *Croat. Chem. Acta* **68** (1995) 53–62.
31. O. Ivanciuc, T. Ivanciuc, and A. T. Balaban, *A C H – Model. Chem*. **137** (2000) 57–82.
32. M. Randić, *New J. Chem*. **21** (1997) 945–951.
33. A. T. Balaban, D. Bonchev, and W. A. Seitz, *J. Mol. Struct. (THEOCHEM)* **280** (1993) 253–260.
34. A. T. Balaban, *MATCH (Commun. Math. Chem.)* **21** (1986) 115–122.
35. O. Ivanciuc, T. Ivanciuc, and A. T. Balaban, *J. Chem. Inf. Comput. Sci.* **38** (1998) 395–401.
36. O. Ivanciuc, T. Ivanciuc, D. Cabrol-Bass, and A. T. Balaban, *J. Chem. Inf. Comput. Sci*. **40** (2000) 732–743.
37. M. D. Wessel and P. C. Jurs, *J. Chem. Inf. Comput. Sci*. **35** (1995) 68–76.
38. S. Liu, C. Cao, and Z. Li, *J. Chem. Inf. Comput. Sci*. **38** (1998) 387–394.
39. Y. Yao, L. Xu, Y. Yang, and X. Yuan, *J. Chem. Inf. Comput. Sci.* **33** (1993) 590–594.
40. L. M. Egolf, M. D. Wessel, and P. C. Jurs, *J. Chem. Inf. Comput. Sci.* **34** (1994) 947–956.
41. M. D. Wessel and P. C. Jurs, *J. Chem. Inf. Comput. Sci.* **35** (1995) 841–850.
42. D. T. Stanton and P. C. Jurs, *J. Chem. Inf. Comput. Sci.* **31** (1991) 301–310.
43. O. Ivanciuc, T. Ivanciuc, and A. T. Balaban, *Tetrahedron* **54** (1998) 9129–9142.
44. A. T. Balaban, L. B. Kier, and N. Joshi, *J. Chem. Inf. Comput. Sci.* **32** (1992) 233–237.
45. A. T. Balaban, S. C. Basak, T. Colburn, and G. D. Grunwald, *J. Chem. Inf. Comput. Sci.* **34** (1994) 1118–1121.
46. J. S. Murray, P. Lane, and P. Politzer, *J. Mol. Struct. (THEOCHEM)* **342** (1995) 15–21.
47. A. T. Balaban, N. Joshi, L. B. Kier, and L. H. Hall, *J. Chem. Inf. Comput. Sci.* **32** (1992) 237–244.
48. A. R. Katritzky, L. Mu, V. S. Lobanov, and M. Karelson, *J. Phys. Chem.* **100** (1996) 10400–10407.
49. A. R. Katritzky, V. S. Lobanov, and M. Karelson, *J. Chem. Inf. Comput. Sci.* **38** (1998) 28–41.
50. S. Wang and G. W. A. Milne, *J. Chem. Inf. Comput. Sci*. **34** (1994) 1242–1250.
51. A. A. Gakh, E. G. Gakh, B. G. Sumpter, and D. W. Noid, *J. Chem. Inf. Comput. Sci*. **34** (1994) 832–839.

52. Z. Mihalić, S. Nikolić, and N. Trinajstić, *J. Chem. Inf. Comput. Sci*. **32** (1992) 28–37.
53. M. Randić, *J. Am. Chem. Soc.* **97** (1975) 6609–6615.
54. S. C. Basak, B. D. Gute, and G. D. Grunwald, *J. Chem. Inf. Comput. Sci.* **36** (1996) 1054–1060.
55. A. T. Balaban, S. C. Basak, and D. Mills, *J. Chem. Inf. Comput. Sci.* **39** (1999) 769–774.
56. R. R. Dreisbach (Ed.), *Physical Properties of Organic Compounds – II*, Advances in Chemistry Series No. 22, Am. Chem. Soc., Washington, DC 1959.
57. R. C. Weast and M. J. Astle, *Handbook of Data on Organic Compounds*, CRC Press, Boca Raton, 1985.
58. T. E. Daubert and R. P. Danner (Eds.), *Design Institute for Physical Property Data (DIPR). Physical and Thermodynamic Properties of Pure Chemicals: Data Compilation,* Vols. 1–4, Hemisphere Publ., New York, 1989.
59. O. Ivanciuc and A. T. Balaban, *Rev. Roum. Chim*. **44** (1999) 479–489.
60. O. Ivanciuc and A. T. Balaban, *Rev. Roum. Chim*. **44** (1999) 539–547.
61. O. Ivanciuc, T. Ivanciuc, D. Cabrol-Bass, and A. T. Balaban, *J. Chem. Inf. Comput. Sci*. **40** (2000) 641–643.
62. O. Ivanciuc, T. Ivanciuc, and A. T. Balaban, work in preparation.
63. O. Ivanciuc, S. L. Taraviras, and D. Cabrol-Bass, *J. Chem. Inf. Comput. Sci*. **40** (2000) 126–134.
64. O. Ivanciuc, T. Ivanciuc, and M. V. Diudea, *Roum. Chem. Quart. Rev*. **7** (1999) 41–67.

SAŽETAK

Obratni Wienerovi indeksi

Alexandru T. Balaban, Denise Mills, Ovidiu Ivanciuc i Subhash C. Basak

Ako se sve topologijske udaljenosti oduzmu od dijametra grafa, dobije se nova simetrijska matrica nazvana obrnuta Wienerova matrica ***RW***. Na glavnoj dijagonali obrnute Wienerove matrice ***RW*** nalaze se nule, a zbrojevi redova ili stupaca matrice daju nove invarijante grafa označene sa σ_i. Polovica svih vrijednosti σ_i nekoga grafa daje novi topologijski indeks (*TI*) nazvan obrnuti Wienerov indeks, Λ. Dane su analitičke formule za σ_i i Λ za nekoliko klasa jednostavnih grafova. Indeks Λ uspoređen je sa srodnim topologijskim indeksima (*TI*). Utvrđeno je da vrijednosti σ_i rastu od periferije prema središtu grafa i da su jednake valencijama vrhova grafa kada je dijametar grafa jednak 2. Proučena je uporabivost obrnutih Wienerovih indeksa u modeliranju odnosa strukture i svojstava molekula. Pokazalo se da ti novi topologijski indeksi dobiveni iz obrnute Wienerove matrice daju bolje modele nego topologijski indeksi izvedeni iz matrice udaljenosti i matrice zaobilaznih udaljenosti.